High-spin study of ^{113}Xe: Smooth band termination in valence space

H. C. Scraggs,[1] E. S. Paul,[1,*] A. J. Boston,[1] C. J. Chiara,[2] M. Devlin,[3,†] O. Dorvaux,[4,‡] D. B. Fossan,[2] P. T. Greenlees,[4] K. Helariutta,[4] P. Jones,[4] R. Julin,[4] S. Juutinen,[4] H. Kankaanpää,[4] H. Kettunen,[4] D. R. LaFosse,[3,§] G. J. Lane,[2,‖] I. Y. Lee,[5] A. O. Macchiavelli,[5] M. Muikku,[4] P. Nieminen,[4] P. Rahkila,[4] D. G. Sarantites,[3] J. M. Sears,[2] A. T. Semple,[1] J. F. Smith,[2,¶] K. Starosta,[2,**] and O. Stezowski[1,††]

[1]*Oliver Lodge Laboratory, University of Liverpool, P.O. Box 147, Liverpool L69 7ZE, United Kingdom*

[2]*Department of Physics and Astronomy, State University of New York at Stony Brook, Stony Brook, New York 11794-3800*

[3]*Department of Chemistry, Washington University, St. Louis, Missouri 63130*

[4]*Department of Physics, University of Jyväskylä, P.O. Box 35, FIN-40351, Jyväskylä, Finland*

[5]*Nuclear Science Division, Lawrence Berkeley National Laboratory, Berkeley, California 94720*

(Received 16 February 2000; published 19 May 2000)

High-spin states have been populated in $^{113}_{54}$Xe using the ^{58}Ni(^{58}Ni,2pn) reaction. A backed-target experiment, at a low beam energy of 210 MeV, was performed using the JUROSPHERE spectrometer, while a thin-target experiment at 250 MeV was performed using the GAMMASPHERE spectrometer in conjunction with the MICROBALL charged-particle detector array and a neutron-detector array. Several new band structures have been identified, one of which exhibits characteristics of smooth termination at high spin.

PACS number(s): 27.60.+j, 21.10.Re

I. INTRODUCTION

$^{113}_{54}Xe_{59}$ is the lightest odd-A xenon isotope for which γ-ray transitions are currently known; the low-spin negative-parity yrast band was established using the technique of recoil-decay tagging (RDT) [1]. The light xenon isotopes are of interest for two main reasons. First, the proximity to the $N=Z=50$ shell closures restricts the amount of angular momentum available to the valence particles, allowing band-termination effects to be observed at experimentally accessible spin values ($30-50\hbar$) [2–4]. Second, both proton and neutron $h_{11/2}$ and $d_{5/2}$ orbitals are near the Fermi surface. These orbitals with $\Delta j=\Delta l=3$ are predicted to induce octupole correlations in light barium ($Z=56$) and xenon ($Z=54$) isotopes which are at a maximum for $N\approx 56$ [5,6], and which may be further enhanced by rapid rotation [7]. Indeed, such effects have been discussed for light xenon isotopes [3,8,9].

The present paper documents new results for ^{113}Xe obtained from two complementary ^{58}Ni+^{58}Ni experiments. The first employed a backed target to maintain good γ-ray energy resolution, while the second used a thin target to investigate high-spin properties. The latter experiment also employed charged-particle and neutron ancillary detectors, which were used to preferentially select γ rays in ^{113}Xe ($2pn$ channel). Several new band structures have been identified, one of which exhibits characteristics of smooth band termination at high spin. No evidence has been found, however, for enhanced $E1$ strength associated with octupole correlations.

II. EXPERIMENTAL DETAILS

Two ^{58}Ni+^{58}Ni experiments were performed using the JUROSPHERE and GAMMASPHERE spectrometers. The former experiment employed a backed target and was sensitive to low-spin properties (stopped γ-ray transitions). The latter experiment used a thin target and was sensitive to high-spin properties (fast γ-ray transitions).

A. Backed-target experiment

A ^{58}Ni beam, supplied by the K130 cyclotron at the accelerator laboratory of the University of Jyväskylä (JYFL), Finland, bombarded a ^{58}Ni target foil of thickness 600 μg/cm^2 backed by 17 mg/cm^2 of ^{197}Au. The backed target was employed to stop the recoiling nuclei, thus eliminating the degradation of the intrinsic γ-ray energy resolution due to Doppler effects. This was especially important for this symmetric reaction with a high recoil velocity ($v/c\approx 4.5\%$). The JUROSPHERE γ-ray spectrometer, containing 7 TESSA-type [10], 5 NORDBALL-type [11], and 14 EUROGRAM-type [12] HPGe detectors, each within a bismuth-germanate escape-suppression shield, was used to record γ-ray coincidences of fold two and above. Approximately 3.6×10^8 events were recorded, of which 80% were $\gamma\gamma$ and 16% $\gamma\gamma\gamma$ coincidences. A two-dimensional matrix

*Corresponding author. Electronic address: esp@ns.ph.liv.ac.uk

†Present address: LANSCE-3, Los Alamos National Laboratory, Los Alamos, NM 87545.

‡Present address: Institut de Recherches Subatomiques, F-67037-Strasbourg Cedex 2, France.

§Present address: Department of Physics and Astronomy, State University of New York at Stony Brook, Stony Brook, NY 11794-3800.

‖Present address: Nuclear Science Division, Lawrence Berkeley National Laboratory, Berkeley, CA 94720.

¶Present address: Schuster Laboratory, University of Manchester, Brunswick Street, Manchester M13 9PL, UK.

**On leave from: Institute of Experimental Physics, Warsaw University, Hoża 69, 00-681 Warsaw, Poland.

††Present address: IPN Lyon, IN2P3-CNRS, Université C. Bernard Lyon-1, F-69622 Villeurbanne Cedex, France.

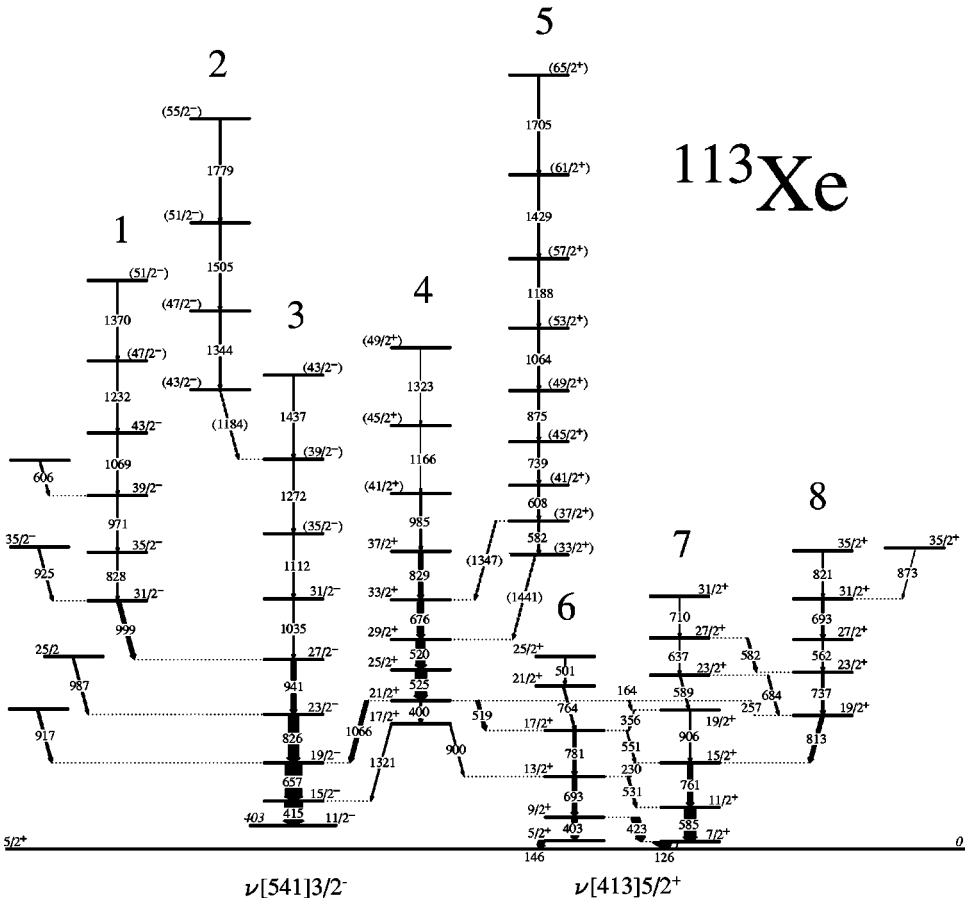

FIG. 1. Level scheme deduced for ^{113}Xe from this work. The transition energies are given in keV and their relative intensities are proportional to the widths of the arrows. Absolute spin/parity assignments are based on systematics.

and a three-dimensional cube were built from the data and analyzed using the RADWARE graphical analysis package [13].

B. Thin-target experiment

This experiment was carried out at the 88-Inch Cyclotron of the Lawrence Berkeley National Laboratory. High-spin states in $A\sim110$ nuclei were populated with the ^{58}Ni(^{58}Ni, $x\alpha\ yp\ zn\ \gamma$) fusion-evaporation reaction at 250 MeV. The beam was incident on two self-supporting nickel targets, each of nominal thickness 500 μg/cm^2. The GAMMASPHERE [14] γ-ray spectrometer, containing 83 HPGe detectors, was used in conjunction with the MICROBALL [15] charged-particle detector and an array of 15 neutron detectors in order to provide clean exit-channel selection by determining the number of evaporated particles (x,y,z). Experimental details are discussed more thoroughly in Ref. [16].

A total of 1.4×10^9 events were recorded with approximately 10^6 events selected off-line for the $2pn$ exit channel (^{113}Xe). Despite the low number of events, the selected data were extremely clean, with an average γ-ray fold of 3.5. These events were unfolded into a RADWARE-format [13] matrix ($\gamma\gamma$) and cube ($\gamma\gamma\gamma$) for subsequent level-scheme construction.

III. RESULTS

The level scheme deduced for ^{113}Xe from this work is shown in Fig. 1, where the ordering of transitions is based on relative γ-ray intensities and triple (γ^3) coincidence relationships. Examples of double-gated γ-ray coincidence spectra, extracted from the backed-target data are presented in Fig. 2. Measured transition energies and the relative intensities of the ^{113}Xe γ rays, deduced from the backed-target data set, are listed in Table I. Relative spins and parities were inferred though an angular-correlation analysis [17] as described in Ref. [9]; the results are included in Table I. Absolute spin/parity assignments are made from systematics.

Double-gated γ-ray spectra extracted from the thin-target data set are shown in Fig. 3. Several of the bands in ^{113}Xe have been extended through the observation of high-energy transitions. These transitions have significantly worse energy resolution due to Doppler effects. Hence the high-energy transitions labeled in Figs. 1 and 3, but not included in Table I, are estimated to be accurate to ±1 keV.

A. Bands 1–3: Negative-parity bands

The lower members of band 3 were originally established in ^{113}Xe using the RDT technique [1] and form the negative-parity yrast line at low spin, based on a $\nu h_{11/2}$ intruder orbital. The bandhead of this band is therefore assigned as $I^\pi=11/2^-$, consistent with the systematics of light odd-A xenon isotopes. The bandhead appears to be isomeric and is located 403 keV above the ground state in the proposed level scheme. Using the $M2$ strength from a similar $11/2^-$ isomer in the ^{111}Te isotone [18], a mean lifetime of approximately 5 μs is estimated for this ^{113}Xe $11/2^-$ isomer.

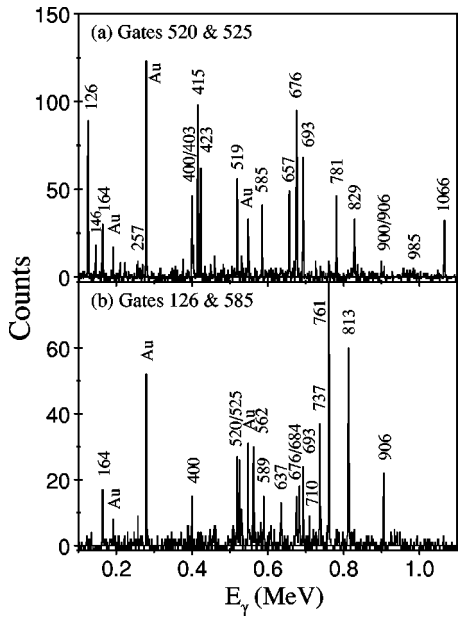

FIG. 2. Examples of gated coincidence spectra, obtained from the cube of the backed-target data, with transition energies labeled in keV: (a) Spectrum double gated by the 520- and 525-keV transitions of band 4. (b) Spectrum double gated by the 126- and 585-keV transitions. Contaminant transitions from the Coulomb excitation of the gold backing are labeled by ''Au.''

Band 1 feeds into band 3 at the $27/2^-$ level. The linking transition has an angular intensity ratio consistent with a stretched quadrupole transition. A weakly populated band of three high-energy γ rays (band 2) feeds band 3 at the $(39/2^-)$ level. It is tentatively linked via the 1184-keV transition of assumed quadrupole multipolarity, see Fig. 3(a).

B. Bands 4–8: Positive-parity bands

Bands 4–8 in Fig. 1 are newly identified, and the positive-parity assignment is consistent with systematics. Band 4 decays into band 3 at the $15/2^-$ and $19/2^-$ levels. The angular-intensity ratios of the linking 1066-keV and 1321-keV transitions imply pure dipole character and an inferred $E1$ multipolarity. Band 4 also decays into bands 6 and 7, which appear as signature partners with interconnecting dipoles. These bands in turn decay into the ground state of ^{113}Xe, which has a proposed spin and parity $I^\pi = 5/2^+$; this assignment is consistent with the ground-state spin and parity assignments of heavier odd-A xenon isotopes.

Band 5 feeds band 4 via tentative high-energy linking transitions, see Fig. 3(b). Band 8 feeds into band 7 and is in turn fed from bands 4 (257-keV transition) and 7.

C. Ratios of reduced transition probabilities

$B(M1;I\rightarrow I-1)/B(E2;I\rightarrow I-2)$ and $B(E1;I\rightarrow I-1)/B(E2;I\rightarrow I-2)$ ratios of reduced transition probabilities may be readily extracted from experimental γ-ray branching ratios of competing $\Delta I=1$ and $\Delta I=2$ transitions. Values extracted for ^{113}Xe were obtained with the procedure detailed in Ref. [3]. For bands 6 and 7, values of $B(M1)/B(E2)\approx 0.40\ (\mu_N/eb)^2$ were found. For the 1066-keV transition linking bands 2 and 3, a value of $B(E1)/B(E2)\approx 10^{-8}$ fm^{-2} was found, which translates into a $B(E1)$ strength of the order of 10^{-5} W.u. for ^{113}Xe when taking the quadrupole deformation, and hence $B(E2)$ strength, from theory (see Sec. IV A).

IV. DISCUSSION

A. Band assignments

Deformation self-consistent cranking calculations based on the total-Routhian surface (TRS) formalism [19–21], employing a triaxial Woods-Saxon single-particle potential [22,23], have been performed for ^{113}Xe. Cranked Woods-Saxon calculations have also been performed using the deformation parameters (β_2, β_4, γ) obtained from the TRS calculations. In all of these calculations, the pairing strength has been calculated at zero frequency and is modeled to decrease with increasing rotational frequency, such that it has fallen by 50% at $\omega=0.70$ MeV/$\hbar$, as detailed in Ref. [20].

A typical quasiparticle diagram is shown in Fig. 4, using the average deformation parameters appropriate for the $(\pi,\alpha)=(-,-1/2)$ configuration, namely $\beta_2=0.200$, $\beta_4=0.040$, and $\gamma=0°$. Band 3 corresponds to the odd neutron occupying orbital e derived from the $\nu h_{11/2}[541]3/2^-$ intruder orbital, while bands 6 and 7 correspond to orbitals a and b, respectively, derived from the $\nu g_{7/2}[413]5/2^+$ Nilsson orbital. The relatively low experimental $B(M1)/B(E2)$ ratios [$\approx 0.40\ (\mu_N/eb)^2$] are consistent with this assignment to a $j=l-1/2$ $\nu g_{7/2}$ orbital, as opposed to a nearby $j=l+1/2$ $\nu d_{5/2}$ orbital. The ground state of ^{113}Xe then most likely corresponds to the occupation of this latter $d_{5/2}$ orbital, namely the $[411]3/2^+$ Nilsson orbital. Note that this orbital is predicted to induce a smaller quadrupole deformation than that used for the calculations shown in Fig. 4.

Rotational alignments of quasiparticle pairs are labeled in Fig. 4. Experimentally, backbends are evident in Fig. 5, which plots the total aligned angular momentum, $I_x=\sqrt{I(I+1)-K^2}$, of the bands in ^{113}Xe as a function of rotational frequency. Backbends occur in the positive-parity bands at $\omega\approx 0.32$ MeV/$\hbar$, which is in good agreement with the predicted neutron alignment ω_{ef} in Fig. 4(b); this backbend is blocked in band 3 due to the occupancy of orbital e. Possible configurations for bands 1 and 2 are three-quasiparticle $\nu[h_{11/2}]\pi[h^2_{11/2}]$ and $\nu[h^3_{11/2}]$ configurations, respectively.

Bands 6 and 7 exhibit the start of a backbend into the $\nu[g_{7/2}h^2_{11/2}]$ three-quasineutron configuration, and thus bands 4 and 8 are best interpreted as signature partners of the $\nu[d_{5/2}h^2_{11/2}]$ configuration. An alternative assignment for band 4 is eEB (see Fig. 4).

B. High-spin properties

The energies of the levels in ^{113}Xe, minus a rigid-rotor reference, are plotted as a function of spin in Fig. 6. The behavior of band 5 at high spin is characteristic of smoothly terminating bands [24] prevalent in this mass region [25]. Based on the systematics of neighboring nuclei [25], the most likely structure of band 5 at high spin is either a

TABLE I. Measured properties of the γ-ray transitions assigned to ^{113}Xe, deduced from the backed-target experiment.

E_γ (keV) [a]	Relative intensity [b]	Angular intensity ratio R [c]	Multipolarity	Assignment	Band [d]
126.0	51	0.72(3)	$M1/E2$	$7/2^+ \rightarrow 5/2^+$	$7 \rightarrow$ g.s.
146.1	8.9	0.62(4)	$M1/E2$	$5/2^+ \rightarrow 5/2^+$	$6 \rightarrow$ g.s.
163.7	5.1	0.56(3)	$M1/E2$	$21/2^+ \rightarrow 19/2^+$	$4 \rightarrow 7$
230.0	4.4	0.64(8)	$M1/E2$	$15/2^+ \rightarrow 13/2^+$	$7 \rightarrow 6$
256.9	1.5	0.79(8)	$M1/E2$	$21/2^+ \rightarrow 19/2^+$	$4 \rightarrow 8$
355.6	2.6	0.72(8)	$M1/E2$	$19/2^+ \rightarrow 17/2^+$	$7 \rightarrow 6$
400.1	9.2	0.95(4)	$E2$	$21/2^+ \rightarrow 17/2^+$	4
402.8	9.0	1.12(16)	$E2$	$9/2^+ \rightarrow 5/2^+$	6
415.2	$\equiv 100$	1.02(3)	$E2$	$15/2^- \rightarrow 11/2^-$	3
423.3	22.4	0.52(2)	$M1/E2$	$9/2^+ \rightarrow 7/2^+$	$6 \rightarrow 7$
500.9	2.4	1.19(9)	$E2$	$25/2^+ \rightarrow 21/2^+$	6
518.6	8.3	0.97(3)	$E2$	$21/2^+ \rightarrow 17/2^+$	$4 \rightarrow 6$
519.6	34.3	1.03(4)	$E2$	$29/2^+ \rightarrow 25/2^+$	4
525.5	43.6	1.02(4)	$E2$	$25/2^+ \rightarrow 21/2^+$	4
530.8	6.9			$13/2^+ \rightarrow 11/2^+$	$6 \rightarrow 7$
551.0	1.2	0.65(15)	$M1/E2$	$17/2^+ \rightarrow 15/2^+$	$6 \rightarrow 7$
562.2	6.2	1.01(8)	$E2$	$27/2^+ \rightarrow 23/2^+$	8
581.9	7.1	0.89(10)	$E2$	$27/2^+ \rightarrow 23/2^+$	$7 \rightarrow 8$
582.4	2.3	0.92(7)	$E2$	$(37/2^+ \rightarrow 33/2^+)$	5
585.2	50	1.13(5)	$E2$	$11/2^+ \rightarrow 7/2^+$	7
589.3	3.8	1.03(10)	$E2$	$23/2^+ \rightarrow 19/2^+$	7
605.9	2.6	0.86(4)		$\rightarrow 39/2^-$	$\rightarrow 1$
607.9	4.9	1.40(12)	$E2$	$(41/2^+ \rightarrow 37/2^+)$	5
637.4	35.4	1.22(4)	$E2$	$27/2^+ \rightarrow 23/2^+$	7
656.7	62.6	1.02(4)	$E2$	$19/2^- \rightarrow 15/2^-$	3
676.3	21.9	1.11(3)	$E2$	$33/2^+ \rightarrow 29/2^+$	4
683.7	12.4	1.09(4)	$E2$	$23/2^+ \rightarrow 19/2^+$	$7 \rightarrow 8$
692.5	10.6	1.20(14)	$E2$	$31/2^+ \rightarrow 27/2^+$	8
693.1	15.3	0.97(3)	$E2$	$13/2^+ \rightarrow 9/2^+$	6
710.3	3.5	0.92(14)	$E2$	$31/2^+ \rightarrow 27/2^+$	7
736.7	11.9	0.92(5)	$E2$	$23/2^+ \rightarrow 19/2^+$	8
739.0	1.2	0.83(8)	$E2$	$(45/2^+ \rightarrow 41/2^+)$	5
761.4	23.0	1.02(6)	$E2$	$15/2^+ \rightarrow 11/2^+$	7
764.4	10.6	1.06(5)	$E2$	$21/2^+ \rightarrow 17/2^+$	6
780.8	14.5	1.03(5)	$E2$	$17/2^+ \rightarrow 13/2^+$	6
812.8	15.9	1.12(6)	$E2$	$19/2^+ \rightarrow 15/2^+$	$8 \rightarrow 7$
820.7	3.0	0.89(9)	$E2$	$35/2^+ \rightarrow 31/2^+$	8
825.6	53.0	1.25(3)	$E2$	$23/2^- \rightarrow 19/2^-$	3
827.7	8.4	1.15(8)	$E2$	$35/2^- \rightarrow 31/2^-$	1
828.9	12.2	0.92(4)	$E2$	$37/2^+ \rightarrow 33/2^+$	1
872.7	2.1	0.96(5)	$E2$	$35/2^+ \rightarrow 31/2^+$	$\rightarrow 8$
874.9	1.2	1.19(14)	$E2$	$(49/2^+ \rightarrow 45/2^+)$	5
899.8	4.9	1.13(9)	$E2$	$17/2^+ \rightarrow 13/2^+$	$4 \rightarrow 6$
906.1	6.3	0.98(7)	$E2$	$19/2^+ \rightarrow 15/2^+$	7
924.8	1.2	0.90(8)	$E2$	$35/2^- \rightarrow 31/2^-$	$\rightarrow 1$
940.6	10.5	1.19(7)	$E2$	$27/2^- \rightarrow 23/2^-$	3
971.2	6.9	0.89(6)	$E2$	$39/2^- \rightarrow 35/2^-$	1
984.6	4.9	1.15(6)	$E2$	$41/2^+ \rightarrow 37/2^+$	4
986.7	7.0	0.64(5)	$\Delta I = 1$	$25/2 \rightarrow 23/2^-$	$\rightarrow 3$
999.2	7.8	1.10(13)	$E2$	$31/2^- \rightarrow 27/2^-$	$1 \rightarrow 3$
1035.1	1.6	1.10(8)	$E2$	$31/2^- \rightarrow 27/2^-$	3

TABLE I. *(Continued.)*

E_γ (keV) [a]	Relative intensity [b]	Angular intensity ratio R [c]	Multipolarity	Assignment	Band [d]
1063.7	2.1			$(53/2^+ \rightarrow 49/2^+)$	5
1066.3	16.4	0.60(4)	$E1$	$21/2^+ \rightarrow 19/2^-$	$4 \rightarrow 3$
1068.6	2.5	0.98(5)	$E2$	$43/2^- \rightarrow 39/2^-$	1
1321.3	1.0	0.67(8)	$E1$	$17/2^+ \rightarrow 15/2^-$	$4 \rightarrow 3$

[a] γ-ray energies are accurate to ± 0.2 keV.
[b] Errors on the relative intensities are estimated to be less than 5% of the quoted values.
[c] The R values were obtained from several spectra gated by the strong low-spin quadrupole transitions. Stretched quadrupole and pure stretched dipole transitions have R values of 1.00 and 0.65, respectively, although pure nonstretched dipole transitions should also have $R \approx 1.00$.
[d] The band numbers correspond to those shown in Fig. 1. ''g.s.'' denotes the ground state.

''valence-space'' [02,2] configuration or a ''core-excited'' [22,2] configuration, using the $[p_1 p_2, n]$ notation of Ref. [26]. Here, p_1 represents the number of $\pi g_{9/2}$ holes, while p_2 and n represent the number of $\pi h_{11/2}$ and $\nu h_{11/2}$ particles, respectively. In the [22,2] configuration, the high-spin structure of band 5 is $\pi[g_{9/2}^{-2} h_{11/2}^2] \nu[h_{11/2}^2]$, with the remaining valence nucleons distributed over $g_{7/2}$ and $d_{5/2}$ orbitals from the $N=4$ oscillator shell; the [02,2] configuration contains no holes in the $\pi g_{9/2}$ subshell. Similar energetically competing valence-space and core-excited configurations have been calculated for other light xenon isotopes [4,26].

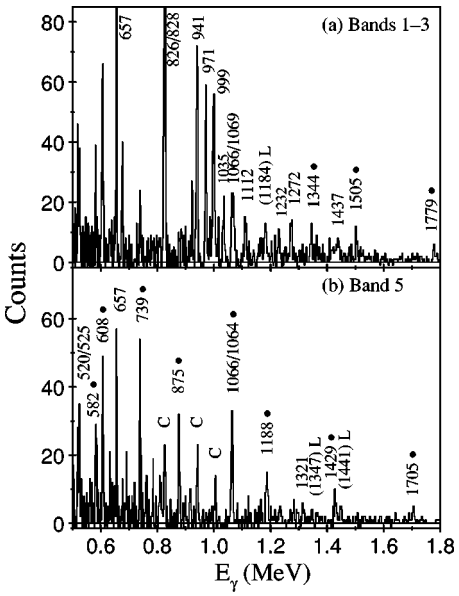

FIG. 3. Examples of gated coincidence spectra, obtained from the cube of the thin-target data, with transition energies labeled in keV: (a) Spectrum gated by all double combinations of transitions of band 3. Members of band 2 are denoted by the solid circles. The tentative 1184-keV link between bands 2 and 3 is labeled ''L.'' (b) Spectrum gated by all double combinations of transitions of band 5. The band members are denoted by the solid circles, the tentative links into band 4 are labeled ''L,'' and contamination peaks are labeled ''C.''

In general, core-excited configurations in xenon isotopes, involving $\pi g_{9/2}$ holes, are predicted to be significantly more deformed than the valence-space configurations, e.g., Ref. [4]. Recent lifetime measurements of high-spin bands in ^{114}Xe [9] and ^{119}Xe [27] favor the less-deformed, valence-space interpretation. Moreover, less spin is available for the valence-space configurations, which therefore terminate at lower spin values than the core-excited configurations. The relatively low-spin ($I \approx 30\hbar$) energy minimum in the rigid-rotor plot for band 5 of ^{113}Xe (Fig. 6) further supports the smoothly terminating valence-space interpretation. Band 5 is thus assigned a [02,2] configuration. A smoothly terminating band in neighboring ^{114}Xe has been assigned a [02,3] configuration [9], while bands in ^{116,118}Xe [2] have been attrib-

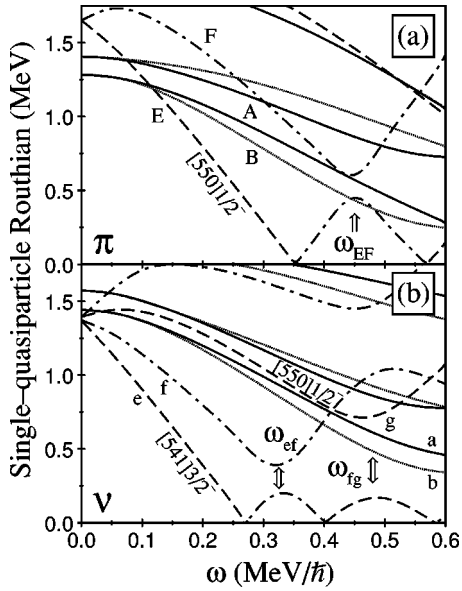

FIG. 4. Representative single-quasiparticle levels for protons (a) and neutrons (b) calculated with a cranked Woods-Saxon potential. The parity and signature (π, α) of the levels are: $(+,+1/2)$, solid lines; $(+,-1/2)$, dotted lines; $(-,-1/2)$, dashed lines; $(-,+1/2)$, dot-dashed lines. The lowest negative-parity intruder levels are labeled by their asymptotic Nilsson quantum numbers, while quasiparticle alignment frequencies are also marked by the arrows.

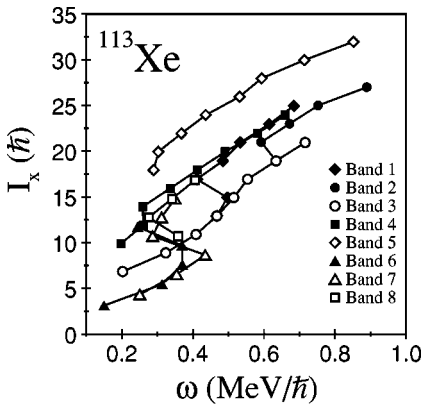

FIG. 5. Total aligned angular momentum, I_x, of the bands in ^{113}Xe, plotted as a function of rotational frequency.

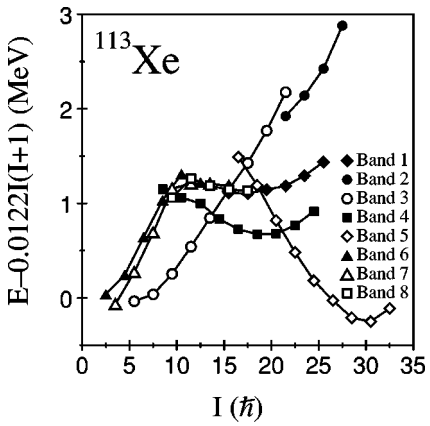

FIG. 6. Energies of the levels in ^{113}Xe, minus a rigid-rotor reference, plotted as a function of spin.

uted to [02,4] configurations, and bands in ^{117,119}Xe [3,4,27] may be associated with [02,5] configurations. Hence the systematics suggest that the $\pi g_{9/2}$ holes do not play a role in smoothly terminating bands in the light xenon ($Z=54$) isotopes. On the other hand, these holes are an essential ingredient of the terminating bands for nuclei with $Z\leqslant 53$, namely iodine, tellurium, antimony, tin, and indium isotopes [25].

C. Octupole correlations?

As the $N=Z$ line is approached, the light xenon isotopes $^{108-114}_{54}$Xe have been predicted to show octupole-correlation effects at low spin [5,6], which may be further enhanced by rapid rotation [7]. Strong $E1$ transitions are a signatures of octupole deformation. The estimated $B(E1)$ strength in ^{113}Xe ($\approx 10^{-5}$ W.u.) is, however, lower than the corresponding values deduced for the heavier, odd-A ^{115,117,121}Xe isotopes (see Fig. 6 of Ref. [3]). Hence it would appear that octupole correlations do not play an important role in ^{113}Xe.

V. CONCLUSIONS

High-spin states have been studied in neutron-deficient ^{113}Xe through complementary backed- and thin-target ^{58}Ni $+^{58}$Ni experiments. Several band structures have been observed to high spin and rotational frequencies. One band, in particular, exhibits characteristics of a smoothly terminating band and extends the systematics of such structures observed in the light xenon isotopes. It is interpreted in terms of a valence-space configuration that does not contain two-particle–two-hole excitations across the spherical $Z=50$ shell gap.

No evidence for enhanced $E1$ strength, and hence strong octupole correlations, was found in this nucleus. Indeed, the estimated $E1$ strength is significantly lower in ^{113}Xe than in heavier odd-A Xe isotopes.

ACKNOWLEDGMENTS

The JUROSPHERE project was supported in part by grants from the U.K. EPSRC and the French IN2P3. Support for this work was also provided by the Academy of Finland and the Large Scale Facility program under the TMR program of the European Union. This work was also supported in part by the U.S. National Science Foundation. The authors are indebted to Dr. D.C. Radford for providing the RADWARE analysis codes, and to Dr. R. Wyss and Dr. W. Nazarewicz for providing the Woods-Saxon cranking codes.

[1] E. S. Paul, P. J. Woods, T. Davinson, R. D. Page, P. J. Sellin, C. W. Beausang, R. M. Clark, R. A. Cunningham, S. A. Forbes, D. B. Fossan, A. Gizon, J. Gizon, K. Hauschild, I. M. Hibbert, A. N. James, D. R. LaFosse, I. Lazarus, H. Schnare, J. Simpson, R. Wadsworth, and M. P. Waring, Phys. Rev. C **51**, 78 (1995).

[2] J. M. Sears, D. B. Fossan, G. R. Gluckman, J. F. Smith, I. Thorslund, E. S. Paul, I. M. Hibbert, and R. Wadsworth, Phys. Rev. C **57**, 2991 (1998).

[3] E. S. Paul, H. C. Scraggs, A. J. Boston, D. B. Fossan, K. Hauschild, I. M. Hibbert, P. J. Nolan, H. Schnare, I. Thorslund, R. Wadsworth, A. N. Wilson, and J. N. Wilson, Nucl. Phys. **A644**, 3 (1998).

[4] H. C. Scraggs, E. S. Paul, A. J. Boston, J. F. C. Cocks, D. M. Cullen, K. Helariutta, P. M. Jones, R. Julin, S. Juutinen, H. Kankaanpää, M. Muikku, P. J. Nolan, C. M. Parry, A. Savelius, R. Wadsworth, A. V. Afanasjev, and I. Ragnarsson, Nucl. Phys. **A640**, 337 (1998).

[5] J. Skalski, Phys. Lett. B **238**, 6 (1990).

[6] P.-H. Heenen, J. Skalski, P. Bonche, and H. Flocard, Phys. Rev. C **50**, 802 (1994).

[7] J. L. Egido and L. M. Robledo, Nucl. Phys. **A494**, 85 (1990).

[8] S. L. Rugari, R. H. France III, B. J. Lund, Z. Zhao, M. Gai, P. A. Butler, V. A. Holliday, A. N. James, G. D. Jones, R. J. Poynter, R. J. Tanner, K. L. Ying, and J. Simpson, Phys. Rev. C **48**, 2078 (1993).

[9] E. S. Paul, H. C. Scraggs, A. J. Boston, O. Dorvaux, P. T. Greenlees, K. Helariutta, P. Jones, R. Julin, S. Juutinen, H. Kankaanpää, H. Kettunen, M. Muikku, P. Nieminen, P. Rahkila, and O. Stezowski, Nucl. Phys. **A673**, 31 (2000).

[10] P. J. Nolan, D. W. Gifford, and P. J. Twin, Nucl. Instrum. Methods Phys. Res. A **236**, 95 (1985).
[11] B. Herskind, Nucl. Phys. **A447**, 395 (1985).
[12] C. W. Beausang, S. A. Forbes, P. Fallon, P. J. Nolan, P. J. Twin, J. N. Mo, J. C. Lisle, M. A. Bentley, J. Simpson, F. A. Beck, D. Curien, G. DeFrance, G. Duchêne, and D. Popescu, Nucl. Instrum. Methods Phys. Res. A **313**, 37 (1992).
[13] D. C. Radford, Nucl. Instrum. Methods Phys. Res. A **361**, 297 (1995); **361**, 306 (1995).
[14] I. Y. Lee, Nucl. Phys. **A520**, 641c (1990).
[15] D. G. Sarantites, P.-F. Hua, M. Devlin, L. G. Sobotka, J. Elson, J. T. Hood, D. R. LaFosse, J. E. Sarantites, and M. R. Maier, Nucl. Instrum. Methods Phys. Res. A **381**, 418 (1996).
[16] A. J. Boston, E. S. Paul, C. J. Chiara, M. Devlin, D. B. Fossan, S. J. Freeman, D. R. LaFosse, G. J. Lane, M. Leddy, I. Y. Lee, A. O. Macchiavelli, P. J. Nolan, D. G. Sarantites, J. M. Sears, A. T. Semple, J. F. Smith, and K. Starosta, Phys. Rev. C **61**, 064305 (2000), this issue.
[17] K. S. Krane, R. M. Steffen, and R. M. Wheeler, Nucl. Data Tables **11**, 351 (1973).
[18] K. Starosta, A. J. Boston, C. J. Chiara, M. Devlin, D. B. Fossan, T. Koike, D. R. LaFosse, G. J. Lane, I. Y. Lee, A. O. Macchiavelli, P. J. Nolan, E. S. Paul, D. G. Sarantites, J. M. Sears, A. T. Semple, and J. F. Smith, Phys. Rev. C **61**, 034308 (2000).
[19] W. Nazarewicz, G. A. Leander, and J. Dudek, Nucl. Phys. **A467**, 437 (1987).
[20] R. Wyss, J. Nyberg, A. Johnson, R. Bengtsson, and W. Nazarewicz, Phys. Lett. B **215**, 211 (1988).
[21] W. Nazarewicz, R. Wyss, and A. Johnson, Nucl. Phys. **A503**, 285 (1989).
[22] W. Nazarewicz, J. Dudek, R. Bengtsson, T. Bengtsson, and I. Ragnarsson, Nucl. Phys. **A435**, 397 (1985).
[23] S. Cwiok, J. Dudek, W. Nazarewicz, W. Skalski, and T. Werner, Comput. Phys. Commun. **46**, 379 (1987).
[24] I. Ragnarsson, V. P. Janzen, D. B. Fossan, N. C. Schmeing, and R. Wadsworth, Phys. Rev. Lett. **74**, 3935 (1995).
[25] A. V. Afanasjev, D. B. Fossan, G. J. Lane, and I. Ragnarsson, Phys. Rep. **322**, 1 (1999).
[26] A. V. Afanasjev and I. Ragnarsson, Nucl. Phys. **A591**, 387 (1995).
[27] H. C. Scraggs, E. S. Paul, A. J. Boston, C. J. Chiara, D. B. Fossan, C. Fox, D. R. LaFosse, P. J. Nolan, T. Koike, K. Starosta, A. Walker, A. V. Afanasjev, and I. Ragnarsson, in *Proceedings of the Conference on Experimental Nuclear Physics in Europe, Sevilla, 1999*, edited by B. Rubio, M. Lozano, and W. Gelletly, AIP Conf. Proc. No. 495 (AIP, New York, 1999), p. 231.